Anthropogenic lead pervasive in Canadian Arctic seawater

Joan De Vera[a], Priyanka Chandan[a], Paulina Pinedo-González[b], Seth G. John[b], Sarah L. Jackson[c,d], Jay T. Cullen[c], Manuel Colombo[e], Kristin J. Orians[e], and Bridget A. Bergquist[a,1]

[a]Department of Earth Sciences, University of Toronto, Toronto, ON M5S 3B1, Canada; [b]Department of Earth Sciences, University of Southern California, Los Angeles, CA 90089; [c]School of Earth and Ocean Sciences, University of Victoria, Victoria, BC V8P 5C2, Canada; [d]Research School of Earth Sciences, The Australian National University, Canberra, ACT 0200, Australia; and [e]Department of Earth, Ocean, and Atmospheric Sciences, University of British Columbia, Vancouver, BC V6T 1Z4, Canada

Edited by Mark Thiemens, University of California San Diego, La Jolla, CA, and approved April 22, 2021 (received for review January 2, 2021)

Anthropogenic Pb is widespread in the environment including remote places. However, its presence in Canadian Arctic seawater is thought to be negligible based on low dissolved Pb (dPb) concentrations and proxy data. Here, we measured dPb isotopes in Arctic seawater with very low dPb concentrations (average ∼5 pmol · kg^{-1}) and show that anthropogenic Pb is pervasive and often dominant in the western Arctic Ocean. Pb isotopes further reveal that historic aerosol Pb from Europe and Russia (Eurasia) deposited to the Arctic during the 20th century, and subsequently remobilized, is a significant source of dPb, particularly in water layers with relatively higher dPb concentrations (up to 16 pmol · kg^{-1}). The 20th century Eurasian Pb is present predominantly in the upper 1,000 m near the shelf but is also detected in older deep water (2,000 to 2,500 m). These findings highlight the importance of the remobilization of anthropogenic Pb associated with previously deposited aerosols, especially those that were emitted during the peak of Pb emissions in the 20th century. This remobilization might be further enhanced because of accelerated melting of permafrost and ice along with increased coastal erosion in the Arctic. Additionally, the detection of 20th century Eurasian Pb in deep water helps constrain ventilation ages. Overall, this study shows that Pb isotopes in Arctic seawater are useful as a gauge of changing particulate and contaminant sources, such as those resulting from increased remobilization (e.g., coastal erosion) and potentially also those associated with increased human activities (e.g., mining and shipping).

anthropogenic lead | lead isotopes | Arctic Ocean | Canada Basin | dissolved lead

Human activities have significantly altered the geochemical cycle of Pb with anthropogenic sources (e.g., leaded gasoline in the 20th century, coal combustion, and smelting) overwhelming natural sources (e.g., crustal particles and volcanic eruptions) (1–3). Anthropogenic Pb is also far reaching because Pb emissions from high-temperature processes can attach, nucleate, and condense to fine aerosol particles, allowing its dispersion over vast distances and deposition in remote places (4, 5). In the ocean, aerosol Pb can enter the water column through a variety of pathways and is redistributed laterally and vertically via ocean circulation. Biogenic (e.g., plankton and organic matter) and authigenic particles also influence the distribution by scavenging the dissolved Pb (dPb), with the estimated dPb residence time in surface waters rich with these particles being shorter (<1 y) (6) than in the deep water (∼100 y) (7, 8) with fewer particles.

Although the Arctic is very remote, anthropogenic Pb from the midlatitude regions reaches the Arctic via atmospheric transport, as evidenced in aerosols (9, 10), snow (11, 12), and ice cores (11, 13, 14). This influx is particularly high during the Arctic haze period (winter and spring) when pollution from Europe and Russia (Eurasia) reaches the Arctic atmosphere (15). Anthropogenic Pb from aerosols can become incorporated in the Arctic Ocean through wet and dry deposition of aerosols (16), resuspension from coasts and shelves, river input, and sea ice melting. However, to date, the atmospheric pathway, which is dominated by anthropogenic Pb (1), is not considered a major source of dPb to the western Arctic Ocean (refer to Fig. 1*A* for the Arctic map). Based on a few proxy measurements from Arctic lake sediments (17), abyssal sediments (18), and Fe–Mn crusts (19) in the western Arctic, major contributions of anthropogenic Pb were not found, and therefore, the contribution of dPb from atmospheric deposition was not considered to be a major source. Abyssal sediments and Fe–Mn crusts in the ocean along with lake sediments are used as proxies to assess the presence of dPb in the water column, because Pb is particle reactive and is readily incorporated in these materials (18, 20). In particular, a study (18) on Pb in abyssal sediments in the Arctic Ocean found evidence of anthropogenic Pb in the abyssal sediments of the eastern but not the western Arctic Ocean. The authors attributed this difference to how Pb is scavenged from Atlantic waters entering the Arctic Ocean. Waters reaching the western Arctic Ocean mainly pass through the highly productive and particle-rich Barents Sea, allowing dPb to be largely scavenged, while waters reaching the eastern Arctic Ocean pass through the Fram Strait and undergo less scavenging (18). With what is assumed to be a limited contribution from anthropogenic Pb, it is thought that dPb in the western Arctic seawater would likely be predominantly natural Pb from coastal and riverine inputs. However,

Significance

Anthropogenic lead (Pb) is widespread and far reaching in the environment. However, it was thought that western Arctic Ocean seawater was pristine based on low dissolved Pb and proxy data. By measuring Pb isotopes on seawater with extremely low concentrations, this study shows that anthropogenic Pb is pervasive in western Arctic Ocean seawater, and much of the dissolved Pb is from remobilization of previously deposited aerosols from the high-Pb emission period of the 20th century. Thus, historic Pb pollution still impacts Arctic seawater, and accelerated melting of permafrost and ice and increased coastal erosion may enhance this remobilization. This study also demonstrates that dissolved Pb isotopes are a sensitive tracer of contaminant and particulate sources in Arctic seawater.

Author contributions: K.J.O. and B.A.B. designed research; J.D.V., P.C., P.P.-G., S.G.J., S.L.J., J.T.C., M.C., K.J.O., and B.A.B. performed research; J.D.V. and B.A.B. analyzed data; P.C., S.L.J., J.T.C., M.C., and K.J.O. participated in the GN03 Canadian Arctic Geotraces cruise and collected samples; J.D.V., P.P.-G., S.G.J., and B.A.B. processed and analyzed the seawater samples for Pb isotope analysis; S.L.J., J.T.C., M.C., and K.J.O., provided the Pb concentration data; and J.D.V. and B.A.B. wrote the paper with assistance from all authors.

The authors declare no competing interest.

This article is a PNAS Direct Submission.

[1]To whom correspondence may be addressed. Email: bergquist@es.utoronto.ca.

This article contains supporting information online at https://www.pnas.org/lookup/suppl/doi:10.1073/pnas.2100023118/-/DCSupplemental.

Published June 14, 2021.

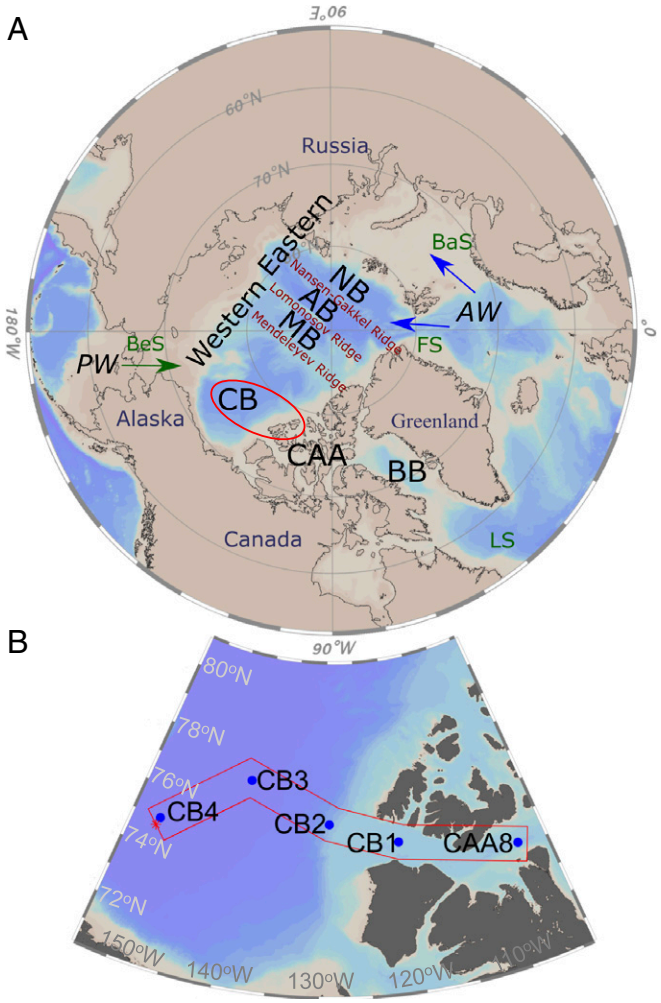

Fig. 1. Maps of the Arctic and the sampling stations (CB1 to CB4 and CAA8). (*A*) The study area (red ellipse) and relevant geographic features in the Arctic based on Rudels (60). The Arctic Ocean has four basins separated by submarine ridges (red text). The CB and Makarov Basin (MB) make up the Western Arctic Ocean, and the Amundsen Basin (AB) and Nansen Basin (NB) make up the Eastern Arctic Ocean. The Pacific-derived water (PW, green arrow) enters Bering Strait (BeS), goes to the CB and MB, and makes up the upper halocline layer. The Atlantic-derived water (AW, blue arrows) enters Fram Strait (FS), and Barents Sea (BaS) travels along the shelves and slopes and reaches all the basins. In the CB, the AW makes up the lower halocline layer, Atlantic water layer, and deep water. The PW from the CB goes to the Canadian Arctic Archipelago (CAA), Baffin Bay (BB), Labrador Sea (LS), and eventually the Atlantic Ocean. (*B*) The sampling locations in the CB are stations CAA8 and CB1 to CB4.

to date, no study has clearly assessed the relative importance of anthropogenic and natural Pb sources directly in Arctic Ocean seawater.

The 2015 Canadian Arctic Geotraces Cruise (GN03) provided an opportunity to measure both dPb and Pb isotopes in seawater samples from the Canada Basin (CB, a part of the western Arctic Ocean; Fig. 1*A*). The dPb data (21) showed extraordinarily low dPb concentrations in the CB, with higher levels of dPb observed in the Pacific-derived water layer, suggesting that some of this dPb came from the Pacific inflow. However, given the very low-Pb concentrations, it was hard to determine the provenance of this Pb from concentrations alone. Thus, we present here Pb isotopes from the same samples (CB1 to CB4 and CAA8 stations collectively referred to as CB; Fig. 1*B*) in order to assess the different sources of Pb in the water column.

Our results show that anthropogenic Pb is pervasive in the Arctic, even at water column depths with low dPb concentrations. We also identified 20th century Eurasian Pb, which is present in different water layers and at depths with relatively higher dPb, as an important component of the dPb. This 20th century Eurasian Pb has a distinctively low $^{206}Pb/^{207}Pb$ ratios, offering insights into the pathway and distribution of anthropogenic Pb in the water column. Our results indicate that remobilization of previously deposited aerosols, especially from the high-Pb emission period (e.g., peak of leaded gasoline in the 20th century), contributes significantly to the dPb budget of the CB.

Results and Discussion

Sources of Pb in the CB. The Pb isotopic compositions of the CB seawater (CB1 to CB4 and CAA8 stations) have a wide range ($^{206}Pb/^{207}Pb$ = 1.131 to 1.195 and $^{208}Pb/^{206}Pb$ = 2.053 to 2.128; Figs. 2 and 3*A* and *SI Appendix*, Table S1) and fall along a mixing line (red line) covering both anthropogenic and natural sources. At the end of the mixing line with low $^{206}Pb/^{207}Pb$ (<1.15), the seawater samples closely match aerosols influenced by European leaded gasoline (22) (Fig. 2, red ellipse). Europe used Pb ore from Broken Hill, Australia, in their leaded gasoline in the 20th century (11), which is characterized by very low $^{206}Pb/^{207}Pb$ (~1.04; after ref. 23). Besides European leaded gasoline, the other possible sources of low $^{206}Pb/^{207}Pb$ from the 20th century (not shown on Fig. 2) are Russian smelters ($^{206}Pb/^{207}Pb$ = ~1.025 to 1.15) (10), Canadian smelters in Quebec and British Columbia ($^{206}Pb/^{207}Pb$ = ~0.99 to 1.07), and Canadian gold mines in Yellowknife ($^{206}/^{207}Pb$ = ~0.95) (24–27). Among these sources, it is likely that both European leaded gasoline and Russian smelters impacted the Arctic, because Eurasian air masses dominate the Arctic's atmosphere during the Arctic haze period (15). This 20th century Eurasian Pb contamination is also supported by the presence of low $^{206}Pb/^{207}Pb$ in Arctic ice core sections between 1920 and 1970 (11) and snow between the 1990s and early 2000s (11).

Canadian and other sources are less likely to be an important source of the low $^{206}Pb/^{207}Pb$ in the Arctic based on what is known about these sources. For example, the Canadian smelters in Quebec and gold mines in Yellowknife had Pb emissions that are more localized (i.e., ~30 to 300 km contamination footprint) (24, 25). Similarly, the Canadian smelters in British Columbia with <1.15 Pb emissions did not dominate the Pb in aerosols (22) and lichens (28) collected in the province, which have a much wider range in $^{206}Pb/^{207}Pb$ (1.14 to 1.19, average = 1.16). In addition, there are recent measurements of low $^{206}Pb/^{207}Pb$ (<1.15) outside the Arctic region from smelters (26, 29–31), unleaded gasoline (30), and possibly leaded gasoline use from select transportation sectors (e.g., aviation fuel) (31). However, Pb from these sources does not appear to be reaching the Arctic based on the higher $^{206}Pb/^{207}Pb$ measured in more modern Arctic aerosols (2010 to 2014; Fig. 2, magenta ellipse).

Although the seawater samples with $^{206}Pb/^{207}Pb > 1.15$ in the middle and high end of the mixing line could be influenced by both anthropogenic and natural sources (Fig. 2), it is likely that many of these samples are still heavily influenced by anthropogenic Pb. Samples with intermediate $^{206}Pb/^{207}Pb$ (~1.15 to 1.17) could reflect the influence of more recent anthropogenic Pb emissions reaching the Arctic with Pb compositions (median $^{206}Pb/^{207}Pb$ = 1.16; after refs. 9 and 32) matching the industrial Pb emissions observed in Europe, Russia, and Canada after the leaded gasoline phaseout in major transportations sectors. Alternatively, the samples with intermediate as well as high $^{206}Pb/^{207}Pb$ (>1.15) may result from the mixing of anthropogenic Pb sources with lower $^{206}Pb/^{207}Pb$ with either natural or anthropogenic sources with higher $^{206}Pb/^{207}Pb$. We tried to quantify the contribution from these sources using a two-component isotope mixing model (Eq. **1**; *Materials and Methods*), assuming that the anthropogenic and natural endmembers

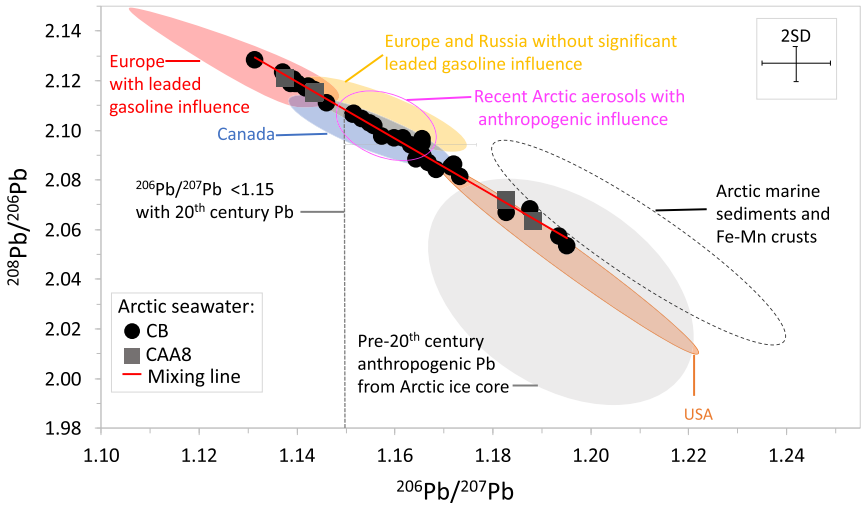

Fig. 2. $^{208}Pb/^{206}Pb$ versus $^{206}Pb/^{207}Pb$ of the CB seawater samples and possible sources. The seawater data (CB1 to CB4 and CAA8) form a mixing line (red line) with influences from anthropogenic and natural sources (ellipses). The anthropogenic emissions are from aerosols, lichens, and precipitation data (1990 to present) in Europe, Russia, Canada, and the USA (22, 28, 61–64). Also shown are the most recent anthropogenic aerosols reaching the Arctic (2010 to 2014) (9, 32) and Pb isotopes from a pre-20th century Arctic ice core (~134 to 4,000 y before present) (13). The isotopic compositions of natural Pb are from Fe–Mn crusts in the CB (19) and marine (65, 66) and river (67) sediments found across the Arctic.

are represented by the lowest and highest $^{206}Pb/^{207}Pb$ measured in the CB, respectively. Based on these assumptions, the anthropogenic Pb content in the CB water column ranged from 7 to 100% with an average of 60% (Fig. 3*B* and *SI Appendix*, Fig. S1), indicating the presence of anthropogenic Pb in the CB at most depths. A sensitivity analysis using other possible endmembers is provided in *SI Appendix*, Table S2.

Distribution of Pb Isotopes and Anthropogenic Pb in the CB. An important finding from this study is the detection of 20th century Eurasian Pb with distinctively low $^{206}Pb/^{207}Pb$ signature (<1.15), which enables us to better understand the pathways and distribution of anthropogenic Pb in the CB. Evidence of 20th century Eurasian Pb is found at different depths, particularly in waters with higher dPb concentrations (*SI Appendix*, Fig. S2) near the shelf above 1,000 m (Figs. 3*A* and 4). Within the upper 1,000 m, the 20th century Eurasian Pb signature is strongest (i.e., highest dPb concentration and lowest $^{206}Pb/^{207}Pb$) over and closest to the shelf (CAA8, CB1, and CB2) and is weaker farther from the shelf. At the more offshore stations (CB3 and CB4), the 20th century Eurasian Pb signature is

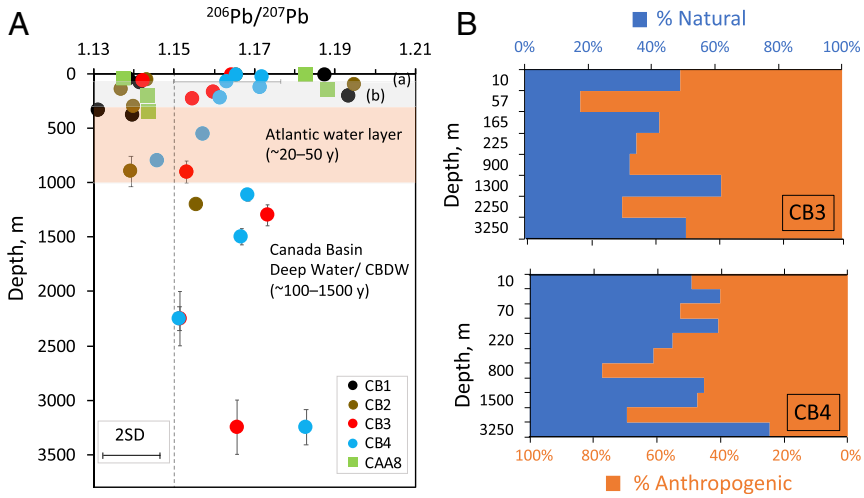

Fig. 3. Depth profiles of the $^{206}Pb/^{207}Pb$ and percentages (%) of anthropogenic and natural Pb estimates in the CB. (*A*) The $^{206}Pb/^{207}Pb$ depth profiles for all the stations are superimposed with water mass layers derived from temperature and salinity (refer to Fig. 1*A* for the origin of the water and *SI Appendix*, Fig. S3 for water mass layer identification from salinity and temperature profiles). The age estimates for each water layer (ages in parenthesis) are based on previous studies (19, 43–45, 68). Water masses are the surface-mixed layer (*a*; above gray), the upper halocline layer containing Pacific-derived water (*b*; gray; ~10 y), the lower halocline and Atlantic layers containing Atlantic-derived water (*c*; orange), and the CB deep water beneath Atlantic water layer. Data points left of the dashed gray line have $^{206}Pb/^{207}Pb$ < 1.1.5. The typical two SD error for $^{206}Pb/^{207}Pb$ for all depths (unless otherwise specified) is represented by the error bar in the lower left corner of the figure. For mixed samples, the average of the mixed depths is plotted in the *y*-axis and the vertical error bars represent the actual depths of the mixed samples (*Materials and Methods* and *SI Appendix*, Table S1). (*B*) The estimated percentage (%) of anthropogenic (orange) and natural (blue) Pb for each depth for the CB3 and CB4 stations, assuming that the anthropogenic and natural endmembers are represented by the lowest and highest $^{206}Pb/^{207}Pb$ measured in the CB, respectively (refer to *Materials and Methods* and *SI Appendix*, Table S2 for a discussion and sensitivity analysis providing ranges of these estimates and *SI Appendix*, Fig. S1 for the CAA8, CB1, and CB2 estimates).

still detected at similar depths as to the stations closer to the shelf, but at lower concentrations and slightly higher $^{206}Pb/^{207}Pb$. Studies in the Arctic show that the shelves are important sources of trace elements [e.g., Fe (33), Zn (34), and Ra (35)] and this is likely true for Pb as well. Shelf- and coastal-related processes (e.g., resuspension of shelf materials, coastal erosion, and melting of sea ice and permafrost), besides being a source of natural Pb, thus appear to remobilize previously deposited 20th century Eurasian Pb contamination as well.

Although it is likely that the elevated Pb in the upper 1,000 m is from remobilization of 20th century Eurasian Pb, contaminant dPb could also come from ocean circulation (i.e., transport via Pacific and Atlantic waters). The upper 1,000 m in the CB consists of the surface-mixed layer (0 to 30 m), the Pacific-derived water layer (~30 to 300 m), and the Atlantic-derived water layer (~300 to 1,000 m; *SI Appendix*, Fig. S3 for details about the different water mass layers in the CB) (36–38). Some of the highest dPb concentrations in the CB are found in the Pacific-derived water layer (21). However, many samples in this water mass (Fig. 3*A* and *SI Appendix*, Fig. S4), particularly those at the same isopycnal surface with the highest dPb concentrations (21), have lower $^{206}Pb/^{207}Pb$ ratios (<1.15) than what might be expected from North Pacific Ocean water, which is characterized by higher $^{206}Pb/^{207}Pb$ values (1.157 to 1.185) (39, 40). For the Atlantic-derived water layer, it is also unlikely that Atlantic water is bringing the Eurasian Pb signatures, since North Atlantic Ocean water also has higher $^{206}Pb/^{207}Pb$ values (1.171 to 1.207) (41, 42). Because ocean circulation cannot bring the lowest $^{206}Pb/^{207}Pb$ compositions (<1.15) to the CB waters, it is more likely that the dPb isotopic minimums in the upper 1,000 m are due to mixing of a low $^{206}Pb/^{207}Pb$ source from the shelf within the Arctic with other Pb sources with higher $^{206}Pb/^{207}Pb$ ratios.

Our study also found 20th century Eurasian Pb in CB deep water below 1,000 m, particularly at depths between 2,000 and 2,500 m, which could help refine the ventilation ages at these depths. Between 1,000 and 2,000 m, the $^{206}Pb/^{207}Pb$ values are higher (1.156 to 1.173), followed by low $^{206}Pb/^{207}Pb$ (~1.15) likely from 20th century Eurasian Pb between 2,000 and 2,500 m, and then are higher again (1.166 to 1.183) from 2,500 to 3,500 m. The three very different Pb isotopic compositions below 1,000 m indicate the presence of at least three different water masses. Studies using ventilations age tracers (e.g., SF_6, CFCs, and CCl_4) (43–45) estimated a wide range of ages (~100 to 1,500 y) at different depths below 1,000 m, albeit with large spatial variability and uncertainties, partly because the concentrations of these tracers were close to the detection limit (43). In particular, the ventilation ages between 2,000 to 2,500 m were estimated between ~100 to 1,000 y old (43–45). Our study, on the other hand, observed 20th century Eurasian Pb at depths of 2,000 to 2,500 m, indicating that the age of this water mass is on the lower end of the current age estimates, since this Pb contaminant cannot be more than 100 y old. Although further studies are needed to investigate how this low $^{206}Pb/^{207}Pb$ was acquired by this deep water, it is possible that this water mass could have had the isotopic composition as a primary signature or could have picked it up when it passed over shallow shelves while entering the Arctic Ocean. Another possibility is that it could be from sinking and advection of cold, dense shelf waters produced from ice formation, although this mechanism has only been observed at shallower depths in coastal polynyas (46) and through modeling (47).

Implications for the Changing Arctic. The dPb concentrations in the Canadian Arctic are generally very low (average ~5 pmol · kg^{-1}), making the Pb concentrations and isotopes in Arctic seawater very sensitive to even small Pb inputs. For example, only 3 pmol · kg^{-1} of a Pb contaminant source with a $^{206}Pb/^{207}Pb$ ratio of ~1.13 (e.g., the 20th century Eurasian Pb) can significantly change the $^{206}Pb/^{207}Pb$ ratio of seawater with a $^{206}Pb/^{207}Pb$ ratio of ~1.20 and dPb concentration of 5 pmol · kg^{-1} to a lower $^{206}Pb/^{207}Pb$ ratio of 1.17. This sensitivity makes Pb and its isotopes in Arctic seawater a useful gauge in identifying particulate and contaminant sources. Prior to this study, it was thought that the contribution to the dPb budget of CB seawater from anthropogenic Pb brought to the Arctic region by atmospheric deposition was negligible (18). However, this work identified the importance of remobilization of previously deposited aerosols from the high-Pb emission period of the 20th century in the dPb in the water column of the Arctic, especially near the shelves where water interacts with coastal sediments. This suggests that remobilization might become a more important source of anthropogenic Pb and other trace elements with the melting of permafrost and icesheets and increased coastal erosion, as has been seen for other elements and contaminants in the polar regions (48, 49). Additionally, Pb isotopes may also be useful in identifying emerging sources of particulate-associated elements and contaminant in the Arctic as the region opens up to more human activities such as mining and shipping (50). Indeed, similar to the observations made by other researchers (51, 52), the Arctic may be envisioned as a "large-scale experiment" for Pb, in which the evolving changes in the region may be witnessed, documented, and used to understand how our activities are impacting the regional environment.

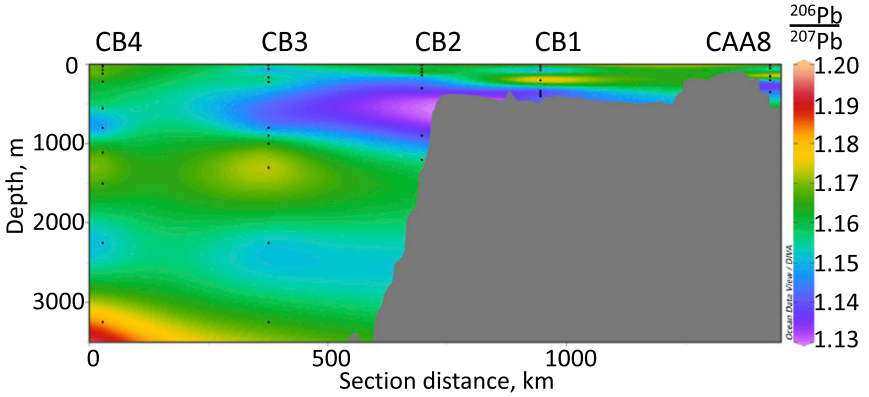

Fig. 4. Interpolated $^{206}Pb/^{207}Pb$ ratios along the CB to CAA8 transect. $^{206}Pb/^{207}Pb$ ratios are depicted by the color bar. The lowest $^{206}Pb/^{207}Pb$ (blue to purple) values, attributed to 20th century Eurasian Pb, are prominently observed near the shelf (CAA8, CB1, and CB2). The simulation was generated using Ocean Data View (69).

Materials and Methods

Sample Locations and Collection. This study is part of the Canadian Arctic Geotraces Cruises (GN02 and GN03) that took place from July 10 to October 1, 2015, aboard Canadian Coast Guard Ship (CCGS) Amundsen. The seawater samples analyzed in this study were from the GN03 cruise collected in the CB (CB1 to CB4) and CAA8 station (Fig. 1*B* and *SI Appendix*, Table S1). All stations (CB1 to CB4 and CAA8) have at least five sampling depths from surface to bottom. The entire study strictly followed trace metal clean protocols and used high-purity acids, reagents, and water (Optima or equivalent brands, 18.2-MΩ Millipore Milli-Q water). The seawater samples were collected using a trace metal clean rosette sampling device based on previously established procedures (53). The rosette system consisted of trace metal clean frame, cables, and twelve 12-L, Teflon-coated Go-Flo bottles (General Oceanics). After sampling, the Go-Flo bottles were moved to a high-efficiency particulate air (HEPA) filtered clean container on the ship, subsampled, and filtered using 0.2-μm Acropak filters (Pall Corporation). The samples were then acidified to pH 1.7 with 12-M, high-purity HCl and processed for Pb isotope measurements at Department of Earth Sciences at University of Toronto.

Sample Processing and Pb Isotopes Measurements. The Arctic seawater samples posed a unique challenge, because the Pb concentrations [complete concentration data and method are reported elsewhere (21, 54, 55)] were very low (average ∼5 pmol · kg^{-1}), and some samples had limited volumes. To overcome this challenge, some of the samples from the same station and adjacent depths (largest depth difference between samples combined was 500 m) were combined in order to have enough Pb for isotopic analysis. Also, the samples in this study were intended for both Pb and Fe (a topic for another study); hence, the previously established method (56) used to process the seawater was modified to allow collection of both metals. The sample processing involved extraction of Pb along with other metals from the seawater samples and then anion exchange chromatography to obtain pure Pb for isotopic measurements.

Extraction and purification. The coextraction of Pb and Fe from seawater was carried out with Nobias PA-1 chelating resin (Hitachi High Technologies) following the method for Fe, Cd, and Zn by Conway et al. (56) Briefly, this method extracted Fe first by adding the resin to the previously acidified seawater sample (∼pH 2) and then mixing the resin–seawater mixture for 2 h to ensure binding of Fe to the resin. Next, the pH of the resin–seawater mixture was increased to ∼6 by adding NH_4OAc buffer solution and 11-M NH_4OH to allow the binding of Pb along with other metals to the resin. The resin was then collected on a 0.4-μm nucleopore filter using a trace metal clean vacuum filter rig (57), and the bound Pb and other metals were eluted from the resin with five aliquots of 5 mL 3-M HNO_3. For samples in which only Pb was extracted, the steps specific for extracting Fe were skipped. The complete extraction procedure is detailed in *SI Appendix*, Fig. S5*A*. The collected eluents were then processed through anion exchange chromatography to obtain pure Fe and Pb.

The overall purification process involved sequential anion exchange chromatography with (1) analytical grade (AG)-MP1 resin to purify Fe (56) and collect Pb and other metals in the non-Fe eluent and (2) AG 1 × 8 resin to purify Pb (58, 59). The purification process began by drying down the eluents from above and then refluxing them in 100 μL each of concentrated HCl and HNO_3 in polytetrafluoroethylene (PTFE) containers for at least 2 h. After drying down the solution, the samples were dissolved with 200 μL 10-M HCl + 0.001% H_2O_2 and ready for the Fe purification step. The HCl solutions were loaded into custom-made PTFE microcolumns with ∼20 μL precleaned AG-MP1 resin. Since AG-MP1 has a weak affinity to Pb in HCl, the solution matrix passing through the column contained Pb and was immediately collected in clean PTFE containers. The column resin and bound Fe were then washed with 100 μL 10-M HCl + 0.001% H_2O_2 and 240 μL 5-M HCl + 0.001% H_2O_2, collecting the washes in the same PTFE containers containing the solution matrix with the Pb. These combined eluents were then evaporated, dried, and dissolved with 2-M HBr for the second column purification with ∼0.3 mL of AG 1 × 8 resin that binds Pb. The column resin and bound Pb were washed with 2 mL 2-M HBr and 2 mL 1.7-M HCl, and then, Pb was eluted with 4 mL 6-M HCl. The eluents containing Pb were dried and dissolved in 2% HNO_3 for Pb isotope analysis. For samples in which only Pb was extracted, the Fe AG-MP1 purification step was skipped. The complete purification procedure is detailed in the schematic diagram (*SI Appendix*, Fig. S5*B*). The estimates of Pb recovery from the first batch of samples (CB3 samples) range from 69 to 140% (median = 107%, $n = 8$). The recoveries above 100% do not necessarily indicate blank contamination, because the procedural blank (median) is only ∼2% of the Pb amount (median) in the final test solutions (refer to *SI Appendix*, Supplementary Text for the discussion of blank). The concentrations for the recovery estimates were approximated from the signal sizes of the final test solutions measured by multicollector inductively coupled plasma mass spectrometer (MC-ICPMS), and hence, they are only rough estimates. Nevertheless, the recovery estimates show that the method extracted the Pb with good recovery from seawater.

Pb isotope measurements. The measurement of Pb isotopes was performed using a Thermo Fisher Scientific Neptune Plus MC-ICPMS. The sample introduction system used was an Apex (Elemental Scientific Inc.) without a desolvator for samples measured between July 2017 and June 2018 and an Aridus II desolvating system (Teledyne CETAC Technologies) for samples measured in October 2018. The X and Jet cones were used to increase the sensitivity, obtaining a ^{208}Pb signal of ∼0.2 V/ppb and ∼0.5 V/ppb for Apex and Aridus systems, respectively. The instrumental mass bias was corrected by using an internal thallium (Tl) standard (National Institute of Standards and Technology [NIST] 997, masses 203 and 205) and bracketing the sample measurements with NIST 981 Pb standards (59). Because of limited sample volumes (at least 0.4-mL final volume), the concentrations of the prepared solutions were not measured prior to the isotope measurements, resulting in sample Pb/Tl and bracketing standard Pb/Tl mismatches of up to 20%. In addition, some of the blanks and samples had a higher Tl signal than what was expected from the spiked Tl, likely due to Tl contamination as the same laboratory uses high-Tl concentrations (NIST 997 also) for mercury isotope measurements. Despite the large mismatches and the presence of some Tl noise, the Pb isotope ratios of the process and instrumental standards (NIST 981 and BCR-2; *SI Appendix*, Table S3) that were run at concentrations and mismatches similar to samples were in agreement with published values. Besides NIST 981 and BCR-2, the data integrity was further assessed by analyzing intercomparison (*SI Appendix*, Table S4) and duplicate (*SI Appendix*, Table S5 seawater samples, and their results are discussed in more detail in *SI Appendix*, Supplementary Text. The errors (two SD) used in this study are ± 0.007 (two SD) for both $^{206}Pb/^{207}Pb$ and $^{208}Pb/^{206}Pb$ (unless otherwise stated) and were based on the intercomparison and the duplicate pairs that had the highest two SDs (excluding the outliers; *SI Appendix*, Supplementary Text).

Two-Component Isotope Mixing Calculation to Estimate the Fractional Contribution of Anthropogenic and Natural Sources. The fractional contribution of anthropogenic (f_a) and natural (f_n) sources of Pb was estimated using a two-endmember mixing model:

$$f_a R_a + f_n R_n = R_{sw}, \quad [1]$$

where the sum of f_a and f_n is one and the Pb isotope ratios of the anthropogenic endmember (*a*), natural endmember (*n*), and seawater sample (*sw*) correspond to R_a, R_n, and R_{sw}, respectively. A sensitivity analysis using two different $^{206}Pb/^{207}Pb$ values for each of the chosen anthropogenic and natural endmembers are provided in *SI Appendix*, Table S2. The selection of the Pb isotope ratios for each endmember are also explained in detail in *SI Appendix*, Table S2.

Data Availability. All study data are included in the article and/or *SI Appendix*.

ACKNOWLEDGMENTS. This research was supported by the Natural Sciences and Engineering Research Council of Canada Climate Change and Atmospheric Research Program (grant: Canadian Arctic-Geotraces Program). We thank the captain and crew of the CCGS Amundsen; the science crew of the Canadian Arctic Geotraces program led by Dr. Roger Francois (chief scientist) for their assistance in the sample collection; Hong Li for assistance in the laboratory; Dr. Don Davis for discussions and insights into Pb isotopes; and Dr. Edward Boyle for providing the intercalibration samples.

1. J. O. Nriagu, J. M. Pacyna, Quantitative assessment of worldwide contamination of air, water and soils by trace metals. *Nature* **333**, 134–139 (1988).
2. J. M. Pacyna, E. G. Pacyna, An assessment of global and regional emissions of trace metals to the atmosphere from anthropogenic sources worldwide. *Environ. Rev.* **9**, 269–298 (2001).
3. J. O. Nriagu, A global assessment of natural sources of atmospheric trace metals. *Nature* **338**, 47–49 (1989).
4. R. A. Duce *et al.*, The atmospheric input of trace species to the world ocean. *Global Biogeochem. Cycles* **5**, 193–259 (1991).
5. D. J. Cziczo *et al.*, Inadvertent climate modification due to anthropogenic lead. *Nat. Geosci.* **2**, 333–336 (2009).
6. M. Chen *et al.*, Importance of lateral transport processes to ^{210}Pb budget in the eastern Chukchi Sea during summer 2003. *Deep Sea Res. Part II Top. Stud. Oceanogr.* **81–84**, 53–62 (2012).

7. M. P. Bacon, D. W. Spencer, P. G. Brewer, $^{210}Pb/^{226}Ra$ and $^{210}Po/^{210}Pb$ disequilibria in seawater and suspended particulate matter. *Earth Planet. Sci. Lett.* **32**, 277–296 (1976).
8. Y. Nozaki, J. Thomson, K. K. Turekian, The distribution of ^{210}Pb and ^{210}Po in the surface waters of the Pacific Ocean. *Earth Planet. Sci. Lett.* **32**, 304–312 (1976).
9. A. Bazzano, D. Cappelletti, R. Udisti, M. Grotti, Long-range transport of atmospheric lead reaching Ny-Ålesund: Inter-annual and seasonal variations of potential source areas. *Atmos. Environ.* **139**, 11–19 (2016).
10. W. T. Sturges, L. A. Barrie, Stable lead isotope ratios in arctic aerosols: Evidence for the origin of arctic air pollution. *Atmos. Environ.* **23**, 2513–2519 (1989).
11. W. Shotyk *et al*., Predominance of industrial Pb in recent snow (1994–2004) and ice (1842–1996) from Devon Island, Arctic Canada. *Geophys. Res. Lett.* **32**, L21814 (2005).
12. K. J. R. Rosman, W. Chisholm, C. F. Boutron, J. P. Candelone, U. Görlach, Isotopic evidence for the source of lead in Greenland snows since the late 1960s. *Nature* **362**, 333–335 (1993).
13. J. Zheng, W. Shotyk, M. Krachler, D. A. Fisher, A 15,800-year record of atmospheric lead deposition on the Devon Island Ice Cap, Nunavut, Canada: Natural and anthropogenic enrichments, isotopic composition, and predominant sources. *Global Biogeochem. Cycles* **21**, 1–11 (2007).
14. S. Hong, J.-P. Candelone, C. C. Patterson, C. F. Boutron, Greenland ice evidence of Hemispheric lead pollution two millennia ago by Greek and Roman Civilizations. *Science* **265**, 1841–1843 (1994).
15. K. S. Law, A. Stohl, Arctic air pollution: Origins and impacts. *Science* **315**, 1537–1540 (2007).
16. C. M. Marsay *et al*., Concentrations, provenance and flux of aerosol trace elements during US GEOTRACES Western Arctic cruise GN01. *Chem. Geol.* **502**, 1–14 (2018).
17. P. Outridge, M. H. Hermanson, W. L. Lockhart, Regional variations in atmospheric deposition and sources of anthropogenic lead in lake sediments across the Canadian Arctic. *Geochim. Cosmochim. Acta* **66**, 3521–3531 (2002).
18. C. Gobeil, R. W. Macdonald, J. N. Smith, L. Beaudin, Atlantic water flow pathways revealed by lead contamination in Arctic basin sediments. *Science* **293**, 1301–1304 (2001).
19. V. Dausmann, M. Frank, C. Siebert, M. Christl, J. R. Hein, The evolution of climatically driven weathering inputs into the western Arctic Ocean since the late Miocene: Radiogenic isotope evidence. *Earth Planet. Sci. Lett.* **419**, 111–124 (2015).
20. A. Veron, C. E. Lambert, A. Isley, P. Linet, F. Grousset, Evidence of recent lead pollution in deep north-east Atlantic sediments. *Nature* **326**, 278–281 (1987).
21. M. Colombo, B. Rogalla, P. G. Myers, S. E. Allen, K. J. Orians, Tracing dissolved lead sources in the Canadian Arctic: Insights from the Canadian GEOTRACES program. *ACS Earth Space Chem.* **3**, 1302–1314 (2019).
22. A. Bollhöfer, K. J. R. Rosman, Isotopic source signatures for atmospheric lead: The Northern Hemisphere. *Geochim. Cosmochim. Acta* **65**, 1727–1740 (2001).
23. B. L. Gulson, Uranium-lead and lead-lead investigations of minerals from the Broken Hill lodes and mine sequence rocks. *Econ. Geol.* **79**, 476–490 (1984).
24. C. Gallon, A. Tessier, C. Gobeil, R. Carignan, Historical perspective of industrial lead emissions to the atmosphere from a Canadian smelter. *Environ. Sci. Technol.* **40**, 741–747 (2006).
25. N. Pelletier *et al*., Lead contamination from gold mining in Yellowknife Bay (Northwest Territories), reconstructed using stable lead isotopes. *Environ. Pollut.* **259**, 113888 (2020).
26. A. E. Shiel, D. Weis, K. J. Orians, Evaluation of zinc, cadmium and lead isotope fractionation during smelting and refining. *Sci. Total Environ.* **408**, 2357–2368 (2010).
27. D. F. Sangster, P. M. Outridge, W. J. Davis, Stable lead isotope characteristics of lead ore deposits of environmental significance. *Environ. Rev.* **8**, 115–147 (2000).
28. A. Simonetti, C. Gariépy, J. Carignan, Tracing sources of atmospheric pollution in Western Canada using the Pb isotopic composition and heavy metal abundances of epiphytic lichens. *Atmos. Environ.* **37**, 2853–2865 (2003).
29. T. Akerman, G. Spiers, P. Beckett, J. Anderson, F. Caron, Assessment of Airborne lead provenance in Northern Ontario, Canada, using isotopic ratios in snow and *Cladonia rangiferina* lichens. *Water Air Soil Pollut.* **232**, 61 (2021).
30. V. Chrastný *et al*., Unleaded gasoline as a significant source of Pb emissions in the Subarctic. *Chemosphere* **193**, 230–236 (2018).
31. A. E. Shiel, D. Weis, K. J. Orians, Tracing cadmium, zinc and lead sources in bivalves from the coasts of western Canada and the USA using isotopes. *Geochim. Cosmochim. Acta* **76**, 175–190 (2012).
32. J. De Vera, *Tracing the Distribution of Pb and Trace Elements in the Canadian Arctic from the Atmosphere to the Ocean* (University of Toronto, 2020).
33. M. B. Klunder *et al*., Dissolved iron in the Arctic shelf seas and surface waters of the central Arctic Ocean: Impact of Arctic river water and ice-melt. *J. Geophys. Res. Oceans* **117**, C01027 (2012).
34. L. T. Jensen *et al*., Biogeochemical cycling of dissolved zinc in the Western Arctic (Arctic GEOTRACES GN01). *Global Biogeochem. Cycles* **33**, 343–369 (2019).
35. L. E. Kipp, M. A. Charette, W. S. Moore, P. B. Henderson, I. G. Rigor, Increased fluxes of shelf-derived materials to the central Arctic Ocean. *Sci. Adv.* **4**, eaao1302 (2018).
36. F. McLaughlin, K. Shimada, E. Carmack, M. Itoh, S. Nishino, The hydrography of the southern Canada Basin, 2002. *Polar Biol.* **28**, 182–189 (2005).
37. M. Steele *et al*., Circulation of summer Pacific halocline water in the Arctic Ocean. *J. Geophys. Res. Ocean.* **109**, C02027 (2004).
38. A. P. Cid, S. Nakatsuka, Y. Sohrin, Stoichiometry among bioactive trace metals in the Chukchi and Beaufort Seas. *J. Oceanogr.* **68**, 985–1001 (2012).
39. C. M. Zurbrick, C. Gallon, A. R. Flegal, Historic and industrial lead within the Northwest Pacific Ocean evidenced by lead isotopes in seawater. *Environ. Sci. Technol.* **51**, 1203–1212 (2017).
40. J. Wu, R. Rember, M. Jin, E. A. Boyle, A. R. Flegal, Isotopic evidence for the source of lead in the North Pacific abyssal water. *Geochim. Cosmochim. Acta* **74**, 4629–4638 (2010).
41. D. Weiss *et al*., Spatial and temporal evolution of lead isotope ratios in the North Atlantic Ocean between 1981 and 1989. *J. Geophys. Res.* **108**, 3306 (2003).
42. C. M. Zurbrick *et al*., Dissolved Pb and Pb isotopes in the North Atlantic from the GEOVIDE transect (GEOTRACES GA-01) and their decadal evolution. *Biogeosciences* **15**, 4995–5014 (2018).
43. T. Tanhua *et al*., Ventilation of the arctic ocean: Mean ages and inventories of anthropogenic CO2 and CFC-11. *J. Geophys. Res. Oceans* **114**, C01002 (2009).
44. B. Rajasakaren *et al*., Trends in anthropogenic carbon in the Arctic Ocean. *Prog. Oceanogr.* **178**, 102177 (2019).
45. H. Deng, H. Ke, P. Huang, X. Chen, M. Cai, Ventilation time and anthropogenic CO2 in the Bering Sea and the Arctic Ocean based on carbon tetrachloride measurements. *J. Oceanogr.* **74**, 439–452 (2018).
46. P. Winsor, D. C. Chapman, Distribution and interannual variability of dense water production from coastal polynyas on the Chukchi Shelf. *J. Geophys. Res. Oceans* **107**, 16–15 (2002).
47. L. G. Anderson, E. P. Jones, B. Rudels, Ventilation of the Arctic Ocean estimated by a plume entrainment model constrained by CFCs. *J. Geophys. Res. Oceans* **104**, 13423–13429 (1999).
48. J. R. Hawkings *et al*.; SALSA Science Team, Enhanced trace element mobilization by Earth's ice sheets. *Proc. Natl. Acad. Sci. U.S.A.* **117**, 31648–31659 (2020).
49. J. Potapowicz, D. Szumińska, M. Szopińska, Ż. Polkowska, The influence of global climate change on the environmental fate of anthropogenic pollution released from the permafrost: Part I. Case study of Antarctica. *Sci. Total Environ.* **651**, 1534–1548 (2019).
50. S. R. Arnold *et al*., Arctic air pollution: Challenges and opportunities for the next decade. *Elementa* **4**, 1–16 (2016).
51. R. Revelle, H. E. Suess, Carbon dioxide exchange between Atmosphere and Ocean and the question of an increase of Atmospheric CO2 during the past decades. *Tellus* **9**, 18–27 (1957).
52. E. Boyle *et al*., Anthropogenic lead emissions in the Ocean: The evolving global experiment. *Oceanography* **27**, 69–75 (2014).
53. G. A. Cutter *et al*., Sampling and sample-handling protocols for GEOTRACES Cruises (2017). http://dx.doi.org/10.25607/OBP-2. Accessed 31 March 2021.
54. S. Jackson, "The distribution of dissolved cadmium in the Canadian Arctic Ocean," MSc thesis, University of Victoria, Victoria, BC, Canada (2017).
55. S. L. Jackson, J. Spence, D. J. Janssen, A. R. S. Ross, J. T. Cullen, Determination of Mn, Fe, Ni, Cu, Zn, Cd and Pb in seawater using offline extraction and triple quadrupole ICP-MS/MS. *J. Anal. At. Spectrom.* **33**, 304–313 (2018).
56. T. M. Conway, A. D. Rosenberg, J. F. Adkins, S. G. John, A new method for precise determination of iron, zinc and cadmium stable isotope ratios in seawater by double-spike mass spectrometry. *Anal. Chim. Acta* **793**, 44–52 (2013). Correction in: *Anal. Chim. Acta* **801**, 97 (2013).
57. E. A. Boyle, B. A. Bergquist, R. A. Kayser, N. Mahowald, Iron, manganese, and lead at Hawaii Ocean Time-series station ALOHA: Temporal variability and an intermediate water hydrothermal plume. *Geochim. Cosmochim. Acta* **69**, 933–952 (2005).
58. C. A. L. Cheyne, A. M. Thibodeau, G. F. Slater, B. A. Bergquist, Lead isotopes as particulate contaminant tracers and chronostratigraphic markers in lake sediments in northeastern North America. *Chem. Geol.* **477**, 47–57 (2018).
59. M. K. Reuer, E. A. Boyle, B. C. Grant, Lead isotope analysis of marine carbonates and seawater by multiple collector ICP-MS. *Chem. Geol.* **200**, 137–153 (2003).
60. B. Rudels, "Arctic basin circulation" in *Encyclopedia of Ocean Sciences*, S. A. Thorpe, K. K. Turekian Eds. (Elsevier, 2001), pp. 177–187.
61. A. Bollhöfer, K. J. R. Rosman, The temporal stability in lead isotopic signatures at selected sites in the Southern and Northern Hemispheres. *Geochim. Cosmochim. Acta* **66**, 1375–1386 (2002).
62. C. Cloquet, N. Estrade, J. Carignan, Ten years of elemental atmospheric metal fallout and Pb isotopic composition monitoring using lichens in northeastern France. *C. R. Geosci.* **347**, 257–266 (2015).
63. L. S. Sherman, J. D. Blum, J. T. Dvonch, L. E. Gratz, M. S. Landis, The use of Pb, Sr, and Hg isotopes in Great Lakes precipitation as a tool for pollution source attribution. *Sci. Total Environ.* **502**, 362–374 (2015).
64. A. Bollhöfer, K. J. R. Rosman, Lead isotopic ratios in European atmospheric aerosols. *Phys. Chem. Earth Part B Hydrol. Oceans Atmos* **26**, 835–838 (2001).
65. J. Maccali, C. Hillaire-Marcel, C. Not, Radiogenic isotope (Nd, Pb, Sr) signatures of surface and sea ice-transported sediments from the Arctic Ocean under the present interglacial conditions. *Polar Res.* **37**, 1442982 (2018).
66. E. Bazhenova, N. Fagel, R. Stein, North American origin of "pink–white" layers at the Mendeleev Ridge (Arctic Ocean): New insights from lead and neodymium isotope composition of detrital sediment component. *Mar. Geol.* **386**, 44–55 (2017).
67. R. Millot, C.-J. Allègre, J. Gaillardet, S. Roy, Lead isotopic systematics of major river sediments: A new estimate of the Pb isotopic composition of the upper continental crust. *Chem. Geol.* **203**, 75–90 (2004).
68. A. M. Wefing, N. Casacuberta, M. Christl, N. Gruber, J. N. Smith, Circulation timescales of Atlantic Water in the Arctic Ocean determined from anthropogenic radionuclides. *Ocean Sci.* **17**, 111–129 (2021).
69. R. Schlitzer, Data analysis and visualization with Ocean data view. *C. Bull. SCMO* **43**, 9–13 (2015).